

Nitric Oxide Reduction by Carbon Monoxide over Supported Hexaruthenium Cluster Catalysts. 1. The Active Site Structure That Depends on Supporting Metal Oxide and Catalytic Reaction Conditions

Taketoshi Minato,[†] Yasuo Izumi,^{*,‡} Ken-ichi Aika,[†] Atsushi Ishiguro,[‡]
Takayuki Nakajima,[‡] and Yasuo Wakatsuki^{*,‡}

Department of Environmental Chemistry and Engineering, Interdisciplinary Graduate School of Science and Engineering, Tokyo Institute of Technology, 4259 Nagatsuta, Midori-ku, Yokohama 226-8502, Japan, and RIKEN (The Institute of Physical and Chemical Research), 2-1, Hirosawa, Wako, Saitama 351-0198, Japan

Received: February 18, 2003; In Final Form: June 2, 2003

Ruthenium site structures supported on metal oxide surfaces were designed by reacting organometallic Ru cluster $[\text{Ru}_6\text{C}(\text{CO})_{16}]^{2-}$ or $[\text{Ru}_6(\text{CO})_{18}]^{2-}$ with various metal oxides, TiO_2 , Al_2O_3 , MgO , and SiO_2 . The surface Ru site structure, formed under various catalyst preparation and reaction conditions, was investigated by the Ru K-edge extended X-ray absorption fine structure (EXAFS). Samples of $[\text{Ru}_6\text{C}(\text{CO})_{16}]^{2-}/\text{TiO}_2$ (anatase) and $[\text{Ru}_6\text{C}(\text{CO})_{16}]^{2-}/\text{TiO}_2$ (rutile) were found to retain the original Ru_6C framework when heated in the presence of NO (2.0 kPa) or NO (2.0 kPa) + CO (2.0 kPa) at 423 K, i.e., catalytic reaction conditions for NO decomposition. At 523 K, the Ru–Ru bonds of the Ru_6C framework were cleaved by the attack of NO. In contrast, the Ru site became spontaneously dispersed over TiO_2 (anatase). When being supported over TiO_2 (mesoporous), MgO , or Al_2O_3 , the Ru_6C framework split into fragments in gaseous NO or NO + CO even at 423 K. The Ru_6 framework of $[\text{Ru}_6(\text{CO})_{18}]^{2-}$ was found to break easily into smaller ensembles in the presence of NO and/or CO at 423 K on support. Taking into consideration the realistic environments in which these catalysts will be used, we also examined the effect of water and oxygen. When water was introduced to the sample $[\text{Ru}_6\text{C}(\text{CO})_{16}]^{2-}/\text{TiO}_2$ (anatase) at 423 K, it did not have any effects on the stabilized Ru_6C framework structure. In the presence of oxygen gas, however, the Ru hexanuclear structure decomposed into isolated Ru cations bound to surface oxygen atoms of TiO_2 (anatase).

Introduction

A variety of heterogeneous catalysts has been developed to contribute to solve environmental problems.¹ These environmental catalysts often consist of complex chemical contents and in many cases it is not clear which site is responsible for the catalytic performance. Supported cluster catalysts are attractive for its unique and well-defined metal ensemble sites stabilized on surface.² The specific catalysis for the synthesis of chemicals has been reported over supported clusters $[\text{Ru}_6\text{C}]$, $[\text{Ru}_6\text{N}]$, and $[\text{Rh}_{10}\text{Se}]$ prepared from the crystal $[\text{PPN}]_2[\text{Ru}_6\text{C}(\text{CO})_{16}]$ (**1**, $\text{PPN} = (\text{PPh}_3)_2\text{N}$), $[\text{PPN}][\text{Ru}_6\text{N}(\text{CO})_{16}]$, and $[\text{PPN}]_2[\text{Rh}_{10}\text{Se}(\text{CO})_{22}]$ on MgO , La_2O_3 , SiO_2 , Al_2O_3 , TiO_2 , etc.^{3–6} The relationship of the precious metal site structure and its specific catalytic performance was clarified. For example, supported $[\text{Ru}_6\text{C}]/\text{TiO}_2$ catalysts exhibited selective oxygenate (formaldehyde, methanol, and dimethyl ether) synthesis starting from $\text{CO} + \text{H}_2$. The hexanuclear ruthenium unit was retained during the catalytic reaction and reversible cluster framework expansion/contraction was observed by the introduction/evacuation of $\text{CO} + \text{H}_2$.^{3,4} The carbido carbon inside stabilized the Ru_6 framework from inside and played a role of the center of “chemical bond spring”.⁴ The supported $[\text{Rh}_{10}\text{Se}]/\text{TiO}_2$ catalysts showed specific high reactivity for the catalytic ethanol synthesis starting from $\text{CO}_2 + \text{H}_2$. The stabilization effects of the Rh_{10} unit by the interstitial

Se atom were reported on the basis of the Se and Rh K-edge XAFS (X-ray absorption fine structure) analyses.⁶

In general, catalytic decomposition of nitric oxide (NO) is a structure sensitive reaction.² It has been recognized that the catalytic performance (conversion and selectivity) is strongly influenced by the morphology (size and shape) of supported metal. The adsorption and catalytic decomposition of NO over metal cluster catalysts have been reported.^{7–9} Palladium cluster catalysts in H-ZSM-5 exhibited high NO conversion (85.0%) to N_2 in the NO + CH_4 reaction. The correlation between its catalytic performance and the morphology of Pd species was reported by XAFS analyses. Pd^{2+} ions on acidic sites were reported to be catalytically active in the presence of O_2 .⁷ Supported $[\text{Pt}_{12}(\text{CO})_{24}]^{2-}/\text{NaY}$ and $[\text{Pt}_9(\text{CO})_{18}]^{2-}/\text{NaY}$ catalysts showed activity 11–14 times higher compared to the case of conventional $\text{Pt}/\text{Al}_2\text{O}_3$ catalysts for the NO + CO reaction.⁸ An intact Pt_{12} or Pt_9 cluster framework inside the zeolite cage was suggested to be the responsible site for the catalysis.⁹

Although ruthenium is one of the most reactive novel metals (Co, Ru, Rh, Pd, Pt) for the NO decomposition, only a little has been reported about the effects of Ru morphology on the catalytic performance of NO decomposition. At the atmospheric gas pressure conditions of NO (0.5%) + CO (2.0%) at 423–523 K, the conversion to N_2 was faster on $\text{Ru}/\text{Al}_2\text{O}_3$ than in the cases on $\text{Rh}/\text{Al}_2\text{O}_3$, $\text{Pd}/\text{Al}_2\text{O}_3$, or $\text{Pt}/\text{Al}_2\text{O}_3$.¹⁰ Recently, the reactions between Ru carbonyl clusters in solutions and polluting gases (NO, SO_2) have been investigated as models of adsorption and catalytic removal of such gaseous molecules on metal

* Corresponding authors. E-mail: yizumi@chemenv.titech.ac.jp and waky@postman.riken.go.jp.

[†] Tokyo Institute of Technology.

[‡] RIKEN.

ensemble site.^{11–13} Ishiguro et al. recently reported the application of cluster **1** to sulfur dioxide removal by supporting on TiO₂.^{14,15} Crystals of [PPN][Ru₆C(CO)₁₅(NO)] (**2**) were isolated from a reaction mixture obtained by bubbling NO gas through a CH₂Cl₂ solution of complex **1** at room temperature. On further bubbling of NO gas, [PPN][Ru₆C(CO)₁₂(NO)₃] (**3**) and Ru₅C(CO)₁₄(NO)(NO₂) (**4**) were formed. These model reactions show that NO gas can easily substitute a carbonyl ligand of the original hexanuclear Ru cluster even at room temperature, but further addition of NO leads to stepwise cleavage of the metal–metal bond.¹¹ Above 423 K in NO, decomposition of cluster **1** into an ill-defined insoluble precipitate has been noted.

In this paper, the structure of supported [Ru₆C(CO)₁₆]²⁻ clusters is reported to establish the in situ structural benchmark of the application to catalytic reduction of NO. Appropriate inorganic oxide support material was investigated to finely control the surface Ru site structure to be most active for the catalytic removal of NO. To control the Ru site structure and accordingly the catalytic reactivity, major control factors were the basicity/acidity of the support, the extent of saturation of the surface metal site, and the specific surface area of the catalyst.

Experimental Section

Catalysts Preparation. The cluster **1** crystal was prepared by the method described in ref 16. MgO (specific surface area 200 m² g⁻¹) was prepared from Mg(OH)₂ (Wako, 99.99%) by heating at 773 K for 2 h in a vacuum. Al₂O₃ (Aerosil C) (100 m² g⁻¹), anatase (major phase, >83%) TiO₂ (Aerosil P25) (50 m² g⁻¹), rutile (the purity of TiO₂ > 99.8%) TiO₂ (JRC-TIO-3, given by the Catalysis Society of Japan) (51 m² g⁻¹), mesoporous TiO₂ (1 131 m² g⁻¹, given by H. Yoshitake at Yokohama National University), and SiO₂ (Fuji-Silysia C-9709008) (273 m² g⁻¹) were heated at 673 K for 2 h in a vacuum except for the case of mesoporous TiO₂ at 473 K to avoid sintering. Three kinds of TiO₂ are denoted as A-TiO₂, R-TiO₂, and M-TiO₂, respectively. The crystal phase component ratio of A-TiO₂ and R-TiO₂ showed negligible change upon reaction with cluster **1** in a vacuum and in NO and/or CO gas at 423 K, on the basis of the X-ray diffraction (XRD) observations. In the case of M-TiO₂, the XRD data remained unchanged; i.e., it was always in the amorphous state in these reaction conditions. Cluster **1** was reacted with MgO, Al₂O₃, A-TiO₂, R-TiO₂, M-TiO₂, and SiO₂ at 290 K for 2 h in purified tetrahydrofuran (Wako, Special Grade, no stabilizer), and THF was subsequently removed in a vacuum. The loading of Ru was 1.5 wt % for all the samples. The supported carbido Ru clusters are denoted as [Ru₆C]/support.

Noncarbido [PPN]₂[Ru₆(CO)₁₈] (**5**) cluster crystal was prepared by the method described in ref 17. Cluster **5** was supported on A-TiO₂ in THF solution in a manner similar to the case of cluster **1**. This supported Ru cluster is denoted as [Ru₆]/A-TiO₂. The Ru loading was 1.5 wt %.

All the process of cluster catalysts preparation and transfer to reactor or sample cell was carried out in an argon (99.99%) or helium (99.99%) atmosphere. The incipient supported clusters were heated in 2.0 kPa of NO for 30 min at 423–623 K. Alternatively, the supported cluster was heated in NO (2.0 kPa) + CO (2.0 kPa) + O₂ (0.56 kPa) or in NO + CO + H₂O (3.1 kPa) for 3 h at 423 K.

Conventional Ru catalyst was prepared by the impregnation of A-TiO₂ from an aqueous solution of Ru(NO)(NO₃)₃ (Ru 1.5 wt %). Obtained powder was calcined in air at 623 K for 2 h and heated in 20 kPa of H₂ at 623 K for 2 h (denoted as Ru/A-TiO₂).

TABLE 1: Catalytic N₂ Formation Rate at 423 K from NO (2.0 kPa) and CO (2.0 kPa) on [Ru₆C]/Oxides, [Ru₆]/A-TiO₂, and Conventional Ru/A-TiO₂ Catalyst

entry	catalyst	T_{preheat}^a (K)	reaction gas ^b	N ₂ formation rate (10 ⁻⁷ mol of N ₂ min ⁻¹ g of cat. ⁻¹)
a	[Ru ₆ C]/A-TiO ₂	423	NO + CO	5.1
b		523		2.9
c		623		2.5
d		423	NO + CO + H ₂ O (1.7 kPa)	10.9
e		423	NO + CO + O ₂ (0.56 kPa)	2.6
f	[Ru ₆]/A-TiO ₂	423	NO + CO	3.3
g	conv Ru/A-TiO ₂	423	NO + CO	0.41
h	[Ru ₆ C]/Al ₂ O ₃	423		1.6
i	[Ru ₆ C]/MgO	423		1.5
j	[Ru ₆ C]/SiO ₂	423		0.83

^a Catalysts were heated in NO (2.0 kPa) before the catalytic test.

^b The pressure of NO (2.0 kPa) and CO (2.0 kPa) was fixed.

XAFS Measurements. The Ru K-edge XAFS spectra were measured at 290 or 13 K using beamline 10B of the Photon Factory in the National Laboratory for High Energy Physics. The accumulation ring energy was 2.5 GeV, and the ring current was 400–290 mA. The bending-magnet beamline 10B utilized a channel-cut double crystal monochromator of Si(311). Samples were placed vertically. The incident and transmitted X-rays were monitored by ion chambers filled with Ar for I₀ and Kr for I. In situ prepared samples were transferred to a Pyrex glass cell, and transported to the beamline at Tsukuba.

EXAFS Analysis. The EXAFS spectra were analyzed by the program EXAFSH.¹⁸ The postedge background subtraction was performed by calculating the three-block cubic spline, followed by the normalization by using the Victoreen equation. Normalization was performed at $k = 4.0 \text{ \AA}^{-1}$ relative to the derivative maximum of the absorption edge. The Fourier transform of k^3 -weighted χ function was carried out over the range $k_{\text{min}} = 3.0$ and $k_{\text{max}} = 13.0\text{--}14.0 \text{ \AA}^{-1}$ with the window function of 0.5 \AA^{-1} on both sides of the region. The inverse Fourier transform was performed in the filtering range $r = 1.0\text{--}4.5 \text{ \AA}$.

The curve fitting analysis was performed in the range $k_{\text{min}} = 4$ and $k_{\text{max}} = 12.0\text{--}13.0 \text{ \AA}^{-1}$ by the empirical phase shift and amplitude functions extracted from the EXAFS of model compounds: Ru powder for Ru–Ru bond (2.67 Å), RuO₂ powder for Ru–O bond (1.98 Å), Ru₃(CO)₁₂ crystal for Ru–C bond (1.93 Å), [RuCl₂(CO)₃]₂ crystal for Ru(–C–)O bond (3.03 Å), and [PPN]₂[Ru₆C(CO)₁₆] crystal for Ru(–C–)Ru bond (4.09 Å).⁵ The fit quality was evaluated by calculating the *R* factor (*R_f*).

$$R_f = \int |k^3 \chi^{\text{obs}}(k) - k^3 \chi^{\text{calc}}(k)|^2 dk / \int |k^3 \chi^{\text{obs}}(k)|^2 dk$$

Results

Effects of Support. The catalytic reactivity of [Ru₆C]/A-TiO₂ for the NO reduction was preliminarily examined in the heating temperature range 423–623 K (Table 1a–c). Sample [Ru₆C]/A-TiO₂ previously heated in NO at 423 K showed highest activity of N₂ formation as high as 5.1×10^{-7} mol of N₂ min⁻¹ g_{cat}⁻¹ in the NO + CO reaction. In the following structural study, we focused on the TiO₂ case because the catalytic test results were best in the case rather than the cases using other supports (Table 1).

The EXAFS spectrum for [Ru₆C]/A-TiO₂ heated in NO (2.0 kPa) at 423 K is shown in Figure 1. The best-fit result of the

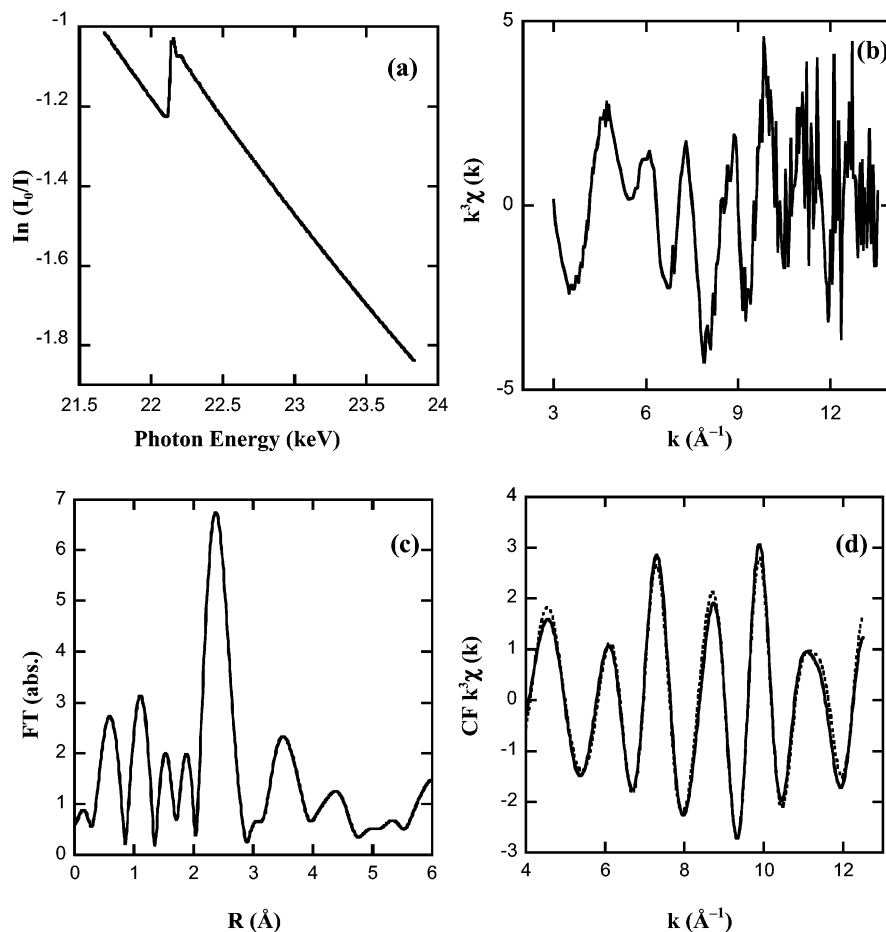


Figure 1. Ru K-edge EXAFS for [Ru₆C]/A-TiO₂ in NO (2.0 kPa) at 423 K: (a) raw spectrum; (b) the k^3 -weighted EXAFS oscillation; (c) its associated Fourier transform; (d) the curve fit analysis. Key: (—) observed; (···) calculated.

TABLE 2: Structural Parameters Based on the Curve Fit Analysis for the Ru K-Edge EXAFS for Supported Ru Cluster Catalysts and Reference Metric Data of Cluster Crystals

entry	catalysts	T_{Preheat}^b (K)	reaction gas ^c	Ru—O			Ru—C or Ru—N			Ru—Ru			Ru(—C—)O or Ru(—N—)O			Ru(—C—)Ru	R_f (%)		
				N	r (Å)	$\Delta(\sigma^2)^a$	N	r (Å)	$\Delta(\sigma^2)^a$	N	r (Å)	$\Delta(\sigma^2)^a$	N	r (Å)	$\Delta(\sigma^2)^a$			N	r (Å)
a	[Ru ₆ C]/A-TiO ₂	423					3.0	1.91	9.0	3.5	2.87	2.1	3.0	3.05	1.4	0.7	3.99	2.3	1.7
b			NO—CO				1.5	2.11	−0.2	3.5	2.87	4.2	2.1	3.08	3.2	0.6	4.05	−0.2	2.6
c			NO—CO—H ₂ O (3.1 kPa)				2.0	2.12	2.8	3.5	2.87	5.6	2.3	3.08	7.3	0.6	4.07	1.4	3.8
d			NO—CO—O ₂ (0.56 kPa)	1.7	2.05	5.9	0.6	1.83	−2.9				0.6	2.94	0.11				4.0
e		523		1.9	2.00	−2.6													2.0
f		623		1.7	2.08	−0.3	0.8	2.02	−1.7	2.4	2.66	4.9	1.0	2.87	2.4				0.0
g	[Ru ₆ C]/R-TiO ₂	423					3.0	1.91	7.4	3.6	2.86	4.9	3.0	3.04	1.5	0.7	4.10	0.6	3.8
h	[Ru ₆ C]/M-TiO ₂			1.8	2.10	2.9	1.0	1.97	5.5	1.4	2.65	9.9	1.4	2.95	5.0				0.2
i	[Ru ₆ C]/SiO ₂						2.5	1.87	1.3	4.1	2.82	2.7	2.5	2.98	0.5	0.8	4.12	0.0	3.5
j			NO—CO	1.3	2.06	−1.7	0.9	2.01	−1.7	4.0	2.65	8.7	0.9	2.89	−0.7	0.3	4.05	−1.7	0.9
k	[Ru ₆ C]/Al ₂ O ₃			1.3	2.03	−3.1	1.0	1.97	−0.9	0.8	2.63	4.6	1.2	2.88	2.5				3.4
l	[Ru ₆ C]/MgO			2.2	2.04	0.1	1.0	1.97	1.1	2.7	2.65	9.1	1.0	2.87	2.6				2.3
m	[Ru ₆]/A-TiO ₂			1.9	2.05	1.6	0.8	1.76	8.7				0.8	2.90	2.0				1.5
n			NO—CO	1.9	2.05	5.7	0.6	1.83	3.3				0.6	2.93	1.5				3.2
o	Ru/A-TiO ₂									11.1	2.68	1.2							0.8
p	[Ru ₆ C(CO) ₁₆] ^{2−d}	—					3.3	1.95		4.0	2.89		3.3	3.03		1.0	4.09		
q	[Ru ₆ C(CO) ₁₂ (NO) ₃] ^{−d}	—					3	1.93		4	2.89		3	3.03		1	4.09		

^a The unit of $\Delta(\sigma^2)$ is 10^{-3} Å². ^b In NO (2.0 kPa) for 30 min. ^c NO (2.0 kPa) and CO (2.0 kPa). Temperature = 423 K. ^d Determined by X-ray crystallographic analysis. The contribution of NO ligand was considered for cluster 3.

curve-fitting analysis for the spectrum is listed in Table 2a. In its associated Fourier transform (Figure 1c), the peaks at 1.3–2.0, 2.3, and 3.5 Å (phase shift uncorrected) were ascribed to Ru—C, Ru—Ru + Ru(—C—)O, and Ru(—C—)Ru bonds, respectively. The first and second peaks also include the contribution of Ru—N and Ru(—N—)O, respectively, because the

average bond length of Ru—N (1.76 Å) is similar to that of Ru—C (1.97 Å) and the average bond length of Ru(—N—)O (3.00 Å) is similar to that of Ru(—C—)O (3.03 Å) for cluster 3.¹⁹ The obtained bond lengths (r) and coordination numbers (N) of Ru—C (1.91 Å with $N = 3.0$), Ru—Ru (2.87 Å with $N = 3.5$), Ru(—C—)O (3.05 Å with $N = 3.0$), and Ru(—C—)Ru

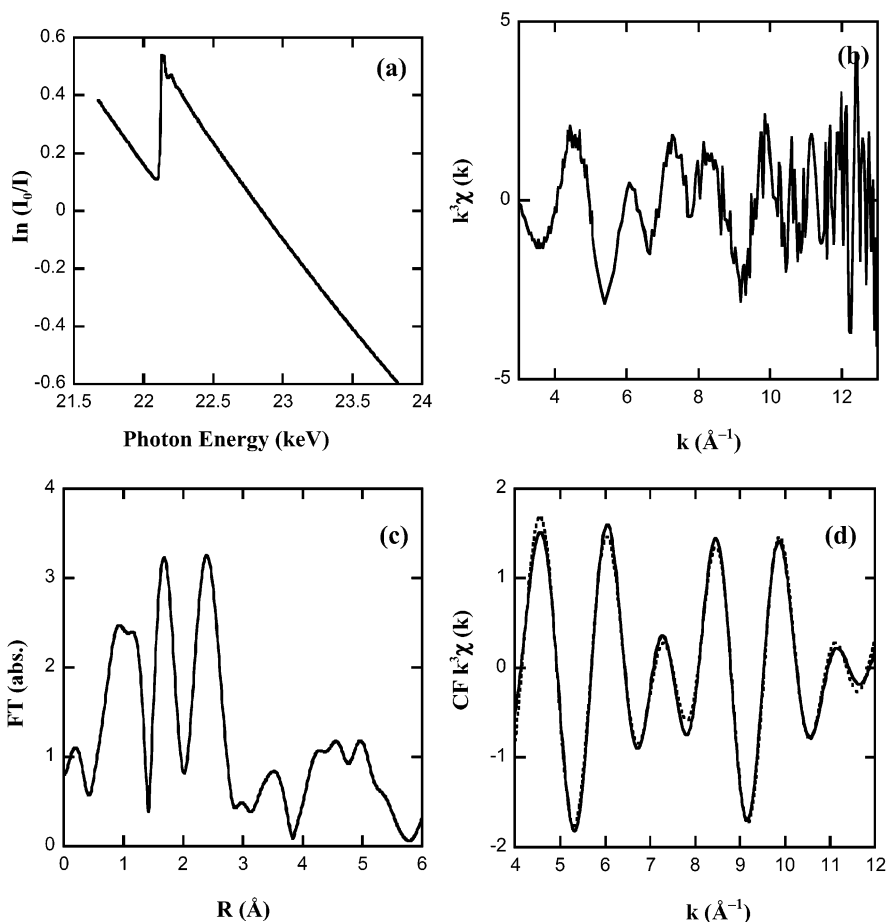


Figure 2. Ru K-edge EXAFS for [Ru₆C]/M-TiO₂ in NO (2.0 kPa) at 423 K: (a) raw spectrum; (b) the k^3 -weighted EXAFS oscillation; (c) its associated Fourier transform; (d) the curve fit analysis. Key: (—) observed; (···) calculated.

(3.99 Å with $N = 0.7$) (Table 2a) were essentially identical to the corresponding values based on XRD crystallographic data of cluster **3** (Table 2q),^{11–13} taking the maximum error of coordination number by EXAFS ($\approx 30\%$) into account. It is known that the intensity of the Ru(–C–)Ru multiple scattering peak is greatly reduced when the Ru₆C framework distorts from octahedral to lower symmetry. According to the symmetry change, the $\theta_{\text{Ru–C–Ru}}$ angle decreases from π .²⁰ This may be the reason that the N for the Ru–C–Ru bond (0.7) was smaller by 30% than the case of cluster **3** crystal.

The EXAFS analysis results of [Ru₆C]/R-TiO₂ heated in NO (2.0 kPa) at 423 K were essentially identical to the above case of [Ru₆C]/A-TiO₂ (Table 2a,g). The numbers of CO and NO ligands that remained in the EXAFS sample of [Ru₆C]/A-TiO₂ were evaluated by the gas chromatograph (GC). They were 12.1 and 1.9, respectively, per one Ru₆C cluster unit. The number of NO is 3 in the crystal of cluster **3**. The GC data suggest that cluster **1** was transformed to cluster **3** by the reaction of NO at 423 K, supported on the TiO₂ surface. The Ru site to accommodate one more NO molecule may be used instead to form bond(s) with surface oxygen atom(s) of TiO₂.

The EXAFS spectrum for [Ru₆C]/M-TiO₂ heated in NO (2.0 kPa) at 423 K is shown in Figure 2. The peak at 3.5 Å in the Fourier transform (c) was not fit well with the empirical parameters of the Ru(–C–)Ru bond (Table 2h). The Ru–Ru bond distance decreased from 2.89 for cluster **1** crystal to 2.65 Å. This value is a typical bond distance for the hcp metallic Ru crystal. On the basis of the bond distance of Ru–Ru first coordination, the peak at 3.5 Å may be due to the next-nearest Ru site.²¹ The obtained N value for Ru–Ru first coordination

was 1.4. The Ru hexanuclear structure framework should have split into smaller fragments in this case.

In the cases of [Ru₆C]/Al₂O₃ and [Ru₆C]/MgO, no peak appeared in the region of Ru(–C–)Ru bond in the k^3 -weighted Fourier transform of EXAFS χ function (not shown). Best fit values are listed in Table 2k,l. On the basis of the $r_{\text{Ru–Ru}}$ values (2.63–2.65 Å) and the N values (0.8–2.7), the smaller Ru cluster split from the six-atom ensemble and/or atomically dispersed Ru cations should be distributed on the Al₂O₃ and MgO surface at 423 K in NO.

In the case of [Ru₆C]/SiO₂ (Table 2i), best-fit result was similar to the case of [Ru₆C]/A-TiO₂ and [Ru₆C]/R-TiO₂ and accordingly to that of the cluster **3** crystal. The GC evaluation of the CO ligand number for the EXAFS sample of [Ru₆C]/SiO₂ was 13.9 per a Ru₆C cluster unit. No NO gas derived from the sample was detected ($< 6 \times 10^{-9}$ mol). The [Ru₆C] cluster supported on SiO₂ retained the Ru₆ framework in NO at 423 K, probably due to the lower reactivity between the cluster and the SiO₂ surface. Essentially intact cluster **1** may remain on the SiO₂ surface. (Structurally) unperturbed cluster **1** is less reactive with NO gas rather than partially decarbonylated cluster.^{3–6}

In summary, the transformation of cluster **1** to **3** was suggested on A-TiO₂ and R-TiO₂ in NO at 423 K. The cleavage of Ru–Ru bond in the Ru₆C cluster was typically observed for [Ru₆C]/M-TiO₂, [Ru₆C]/Al₂O₃, and [Ru₆C]/MgO. The retained Ru₆C framework in the case of [Ru₆C]/SiO₂ was suggested to be nonreactive with the NO gas.

Effects of Heating Temperature in NO. The Fourier transforms of EXAFS spectra for [Ru₆C]/A-TiO₂ in NO (2.0 kPa) at 423–623 K are illustrated in Figure 3. The results of

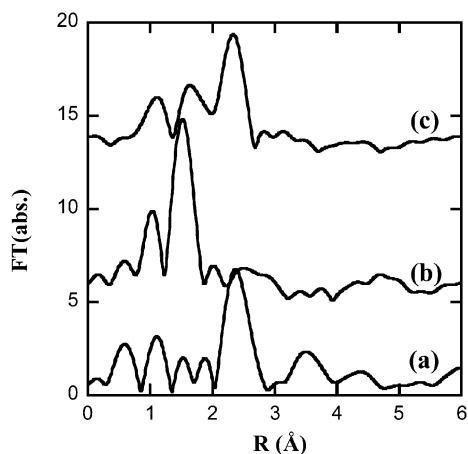


Figure 3. Fourier transforms of k^3 -weighted Ru K-edge EXAFS χ function for $[\text{Ru}_6\text{C}]/\text{A-TiO}_2$ in NO (2.0 kPa) at 423 (a), 523 (b), and 623 K (c).

the curve-fitting analysis are listed in Table 2a,e,f. The result at 423 K was already described in the previous section. The peak originating from Ru(-C-)Ru and Ru-Ru bonds disappeared at 523 K (Figure 3b). All the Ru-Ru bonds in the Ru_6C framework were cleaved and hence the Ru cation was atomically dispersed, stabilized by the bonding with approximately two (in average) surface oxygen atoms at the distance of 2.00 Å. With heating in NO at 623 K, a peak due to Ru-Ru bonds appeared again at 2.4 Å in Figure 3c (phase shift uncorrected). The Ru-Ru first coordination average distance was determined to be 2.66 Å. The diagonal Ru(-C-)Ru coordination peak was

not observed. As the $N_{\text{Ru-Ru}}$ value was as small as 2.4, less than six Ru atoms reconstituted one Ru cluster (unit) in average. The carbido carbon should not remain inside the Ru cluster, and accordingly, the Ru microparticle smaller than 1.0 nm had the metallic nature rather than ruthenium metal carbide.

In summary, retained Ru_6C framework at 423 K entirely split into single Ru cations at 523 K. At 623 K, the metallic Ru cluster was reorganized and the particle size should be very small (smaller than 1.0 nm) because the Ru-Ru coordination number was only 2.4.

Effects of Carbido Carbon. The catalytic reactivity of NO decomposition for noncarbido $[\text{Ru}_6]/\text{A-TiO}_2$ was compared to that of carbido $[\text{Ru}_6\text{C}]/\text{A-TiO}_2$ both heated in the presence of NO (2.0 kPa) at 423 K. The catalytic N_2 formation rate starting from NO + CO gas at 423 K on $[\text{Ru}_6]/\text{A-TiO}_2$ was found to be only 65% of that on $[\text{Ru}_6\text{C}]/\text{A-TiO}_2$ (Table 1a,f). The EXAFS data for $[\text{Ru}_6]/\text{A-TiO}_2$ treated in NO (2.0 kPa) at 423 K are depicted in Figure 4. In our control EXAFS measurement for unsupported cluster 5 crystal, the peak attributed to second nearest Ru-Ru bond (diagonal line of octahedral, 3.96–4.09 Å) was not observed in the Fourier transform of Ru K-edge EXAFS spectrum at 290 K. Due to this reason, only the fit value of the first coordination Ru-Ru peak was used to judge the retention of the Ru_6 framework in the case of supported noncarbido cluster. The best fit consisted of Ru-O, Ru-C (or Ru-N), and Ru(-C-)O (or Ru(-N-)O) (Table 2m). The fit including the Ru-Ru bond contribution was rather worse. A plausible Ru site structure was spontaneously atomically dispersed Ru cations and/or a very small Ru cluster (less than six Ru atoms ensemble) on the TiO_2 surface, in contrast with

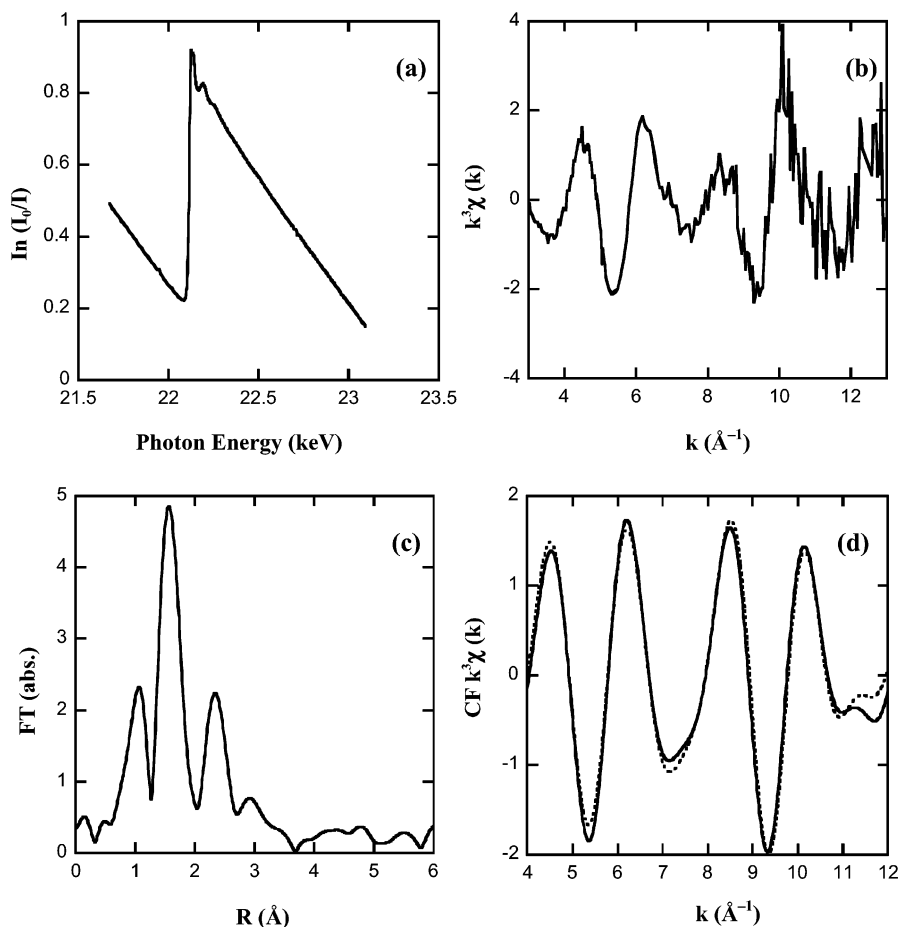


Figure 4. Ru K-edge EXAFS for $[\text{Ru}_6]/\text{A-TiO}_2$ in NO (2.0 kPa) at 423 K: (a) raw spectrum; (b) the k^3 -weighted EXAFS oscillation; (c) its associated Fourier transform; (d) the curve fit analysis. Key: (—) observed (····) calculated.

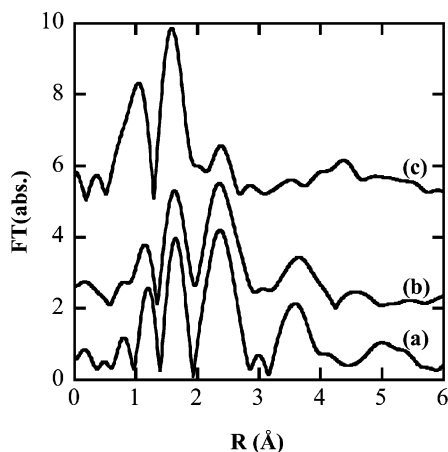


Figure 5. Fourier transforms of k^3 -weighted Ru K-edge EXAFS χ function for [Ru₆C]/A-TiO₂ in NO (2.0 kPa) + CO (2.0 kPa) (a), NO + CO + H₂O (3.1 kPa) (b), and NO + CO + O₂ (0.56 kPa) (c), all at 423 K.

the Ru₆C framework being retained in the case of [Ru₆C]/A-TiO₂ in NO (2.0 kPa) at 423 K.

Ru Site Structure during Catalysis. The Ru cluster site structure of [Ru₆C]/A-TiO₂ was investigated during catalysis in the presence of NO (2.0 kPa) + CO (2.0 kPa) at 423 K. The reaction condition corresponds to the best removal rate of NO in the series of model catalysts (Table 2b). The catalysts under the in situ catalytic reaction condition were quenched and the XAFS spectrum was measured at 290 K. The $N_{\text{Ru}-\text{Ru}}$ and $N_{\text{Ru}(-\text{C})-\text{Ru}}$ values were 3.5 and 0.6, being effectively equivalent to the case of Ru cluster site in only NO at 423 K (3.5 and 0.7, respectively, Table 2a). The addition of gas-phase carbon monoxide did not have significant effects on the Ru cluster structure supported over A-TiO₂.

In contrast, the $N_{\text{Ru}(-\text{C})-\text{Ru}}$ value in the case of [Ru₆C]/SiO₂ in NO (2.0 kPa) + CO (2.0 kPa) at 423 K decreased from 0.8 to 0.3 (Table 2j), suggesting the deformation of Ru octahedral framework. The Ru₆ unit should have contracted to micro-particles of hcp metallic nature on the basis of the obtained Ru–Ru distance of 2.65 Å. The reason of the difference of the Ru site structure is not clear whether in the presence of NO or in the presence of NO + CO (Table 2i,j).

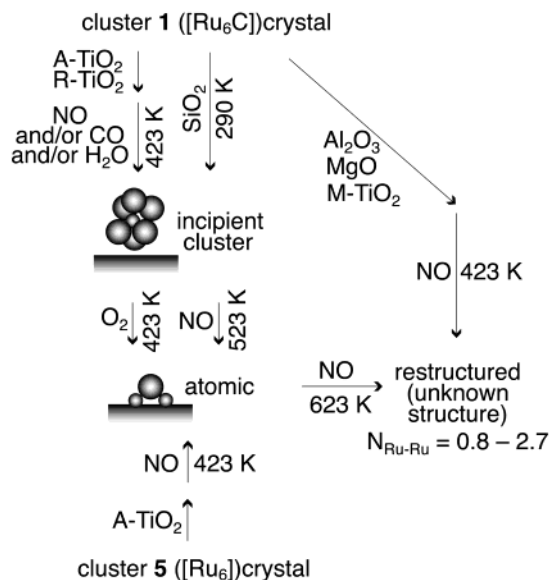
Effects of O₂ and Water. The N₂ formation rate at 423 K starting from NO (2.0 kPa) + CO (2.0 kPa) on [Ru₆C]/A-TiO₂ increased by 112% when 1.7 kPa of water was mixed with the reaction gas (Table 1d). When 0.56 kPa of O₂ was mixed with the reaction gas, the N₂ formation rate decreased by 49% (Table 1e).

Figure 5 compares the Fourier transforms of k^3 -weighted EXAFS χ function in NO + CO (a), in NO + CO + H₂O (b), and in NO + CO + O₂ (c). The results of curve fitting analysis are listed in Table 2a,c,d. Added water did not have a significant effect on the FT data (Figure 5a,b). Upon addition of O₂ to the reaction mixture, the peak around 3.5 Å disappeared and the peak at 2.4 Å became very weak (Figure 5c). The transformed Ru site structure may be similar to that in NO at 523 K (Figure 3b, Table 2e) except that one CO or NO ligand remained to one/two Ru atom(s) when the O₂ gas was introduced to [Ru₆C]/A-TiO₂ at 423 K (Table 2d).

Discussion

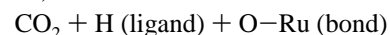
The transformation of the Ru active site is summarized in Scheme 1. The carbido Ru hexanuclear framework was retained at 290 K when cluster 1 was supported on weakly acidic metal

SCHEME 1: Structure Transformation of the Ru Cluster Active Site Based on EXAFS^a



^a The ligand is not drawn for clarity.

oxides such as A-TiO₂, R-TiO₂, and SiO₂. On other supports (M-TiO₂, Al₂O₃, and MgO), the Ru₆C framework appeared to split into smaller fragments on surface. Upon supporting carbonyl clusters on metal oxide, a general reaction we need to assume is the following water gas-shift type.²²



In the cases that this reaction proceeds dominantly, loss of carbonyl ligands should lead to destabilization of the cluster framework. It has been reported that the reactivity of surface hydroxyl group of MgO and Al₂O₃ toward 1 as well as analogous anionic Ru carbonyl clusters is higher than those of TiO₂ and SiO₂ surfaces.^{3,5}

At 423 K in NO, the Ru hexanuclear framework of [Ru₆C]/A-TiO₂ was retained, whereas at 523 K in NO, the cleavage of Ru–Ru bonds occurred and resulted in decomposition of the Ru hexanuclear structure. The effect of carbido carbon in stabilizing the Ru hexanuclear structure of [Ru₆C(CO)₁₆(CH₃)⁻/A-TiO₂ has already been noted either in CO + H₂ or in a vacuum at 523 K.³ In a homogeneous system with saturated NO gas at room temperature, stepwise (partial) cleavage of Ru–Ru bonds in the Ru cluster begins to take place when more than three NO molecules coordinate to the cluster, transforming cluster 1 to 2, and then to 3.¹¹ At higher temperatures of 423–523 K, nearly all the Ru–Ru bonds of cluster 1 were cleaved by the effects of NO and precipitated in solution. In contrast, on the A-TiO₂ surface, a split single (or Ru ensemble consisted of less than six atoms) Ru atom was stabilized by the coordination of surface oxygen atoms (Scheme 1). When heated to 623 K, the Ru–Ru first coordination peak reappeared but the bond distance was shortened by 0.21 Å (Figure 3c, Table 2f).

The overall trend was that the Ru hexanuclear framework became Ru ensemble units of fewer atom numbers (even single Ru atoms) and then the Ru ensemble was reorganized, consisting of fewer than approximately six Ru atoms when the temperature in NO was raised from 423 to 623 K. This trend is understandable to consider the combination of two opposing factors: (1)

the cleavage of Ru–Ru bonds by NO and (2) the higher surface diffusion rate of metal atom (ensemble) at higher temperature. As the temperature was raised, the former factor reduced the Ru ensemble size whereas the latter factor inversely grew the ensemble size. Thus, the Ru ensemble size should reach the minimum at 523 K.

The third and fourth factors are (3) the kind of support and (4) the presence/absence of carbido carbon inside the starting Ru cluster crystal framework. Relatively acidic support and the presence of carbido carbon were found to stabilize the Ru₆ cluster framework. The effects of factors (1), (3) (basic support), and (4) (noncarbido cluster) were dominant in the case on [Ru₆C]/M-TiO₂, Al₂O₃, MgO, and [Ru₆]/A-TiO₂ at 423 K.

Mononuclear surface Ru ion species was suggested as in Scheme 1 in the cases of [Ru₆C]/A-TiO₂ in NO + CO + O₂ at 423 K (Table 2d), [Ru₆C]/A-TiO₂ in NO at 523 K (e), and noncarbido [Ru₆]/A-TiO₂ in NO + CO at 423 K (n). In the presence of CO gas, 0.6 of Ru–C (or Ru–N) and R(–C–)O {or Ru(–N–)O} coordination was observed (Table 2d,n), but only the Ru–O single peak was observed for [Ru₆C]/A-TiO₂ in NO at 523 K (e). Therefore, one CO molecule coordinated to one/two mononuclear surface Ru ion(s). Mononuclear ruthenium carbonyl species, Ru(CO)₂ and Ru(CO)₃ were reported in the case of [Ru(NH₃)₆]/NaY when heated at 393 K.²³ The Ru₃(CO)₁₂ cluster supported in hydroxylated γ -Al₂O₃ was reported to transform into mononuclear [Ru(CO)₂]²⁺ species.²⁴

The Ru metal surface of conventional Ru/TiO₂ catalysts is reported to be predominantly occupied by NO under NO + CO gas.²⁵ In the case of [Ru₆C]/A-TiO₂ (this study), the number of CO and NO ligands was estimated to be 12.1 and 1.9 per one Ru₆C cluster unit on the basis of the EXAFS and GC analysis. The difference of adsorbent (ligand) ratio may be the reason that [Ru₆]/A-TiO₂ exhibited a remarkably higher catalytic NO reduction rate at 423 K than the case of conventional Ru/TiO₂ catalyst (Table 1). The preferable CO adsorption was also reported in the case of [Pt₁₂(CO)₂₄]²⁻/NaY during the NO + CO reaction.^{8,9}

Another plausible explanation of the higher NO reduction rate on [Ru₆C]/A-TiO₂ is the effect of bridging CO (μ_2 -CO) on the Ru cluster site. On conventional Ru catalysts, only terminal (on-top) CO adsorption was observed by FT-IR (Fourier transformed infrared absorption spectroscopy).²⁶ On the contrary, three bridging CO exist in the cluster 3, sharing a common Ru atom with a terminal NO ligand. A similar cluster structure was demonstrated in the case of [Ru₆C]/A-TiO₂ in NO at 423 K (Figure 1 and Table 2a).

In a practical point of view, O₂ and/or H₂O effects were considered. Structural transformation of the ruthenium cluster was observed in the presence of O₂ (Scheme 1), resulting in the partial deactivation of catalytic N₂ formation (Table 1). Water addition exhibited positive effects on this catalysis, however, the reason was not clarified by EXAFS study in this paper.

Conclusions

(1) The Ru hexanuclear framework was retained for [Ru₆C]/A-TiO₂, [Ru₆C]/R-TiO₂, and [Ru₆C]/SiO₂ heated in NO at 423 K. Stabilized Ru hexanuclear structure showed high NO conversion and high N₂ selectivity in the NO + CO reaction at 423 K. The retained Ru₆C core was found to be the best, designed surface site for the environmental NO removal.

(2) The Ru₆ framework stabilized by the effects of carbido carbon and TiO₂ surface split into smaller ensemble and finally

single Ru atoms dispersed on TiO₂ surface until 523 K. This structural transformation was in the negative direction for the catalytic NO decomposition. The dispersed Ru atoms re-organized Ru ensemble consisted of less than six Ru atoms until 623 K.

(3) NO addition and basic support tend to cleave the Ru–Ru bonds. In contrast, carbido carbon stabilized the Ru₆ framework from inside. Elevation of reaction temperature led to the aggregation of Ru atoms.

(4) The addition of O₂ to the reaction mixture NO + CO broke the Ru₆C framework into atomically dispersed Ru atoms. The catalytic reactivity of NO decomposition over the Ru species was lower. No evident structural change was observed by the addition of H₂O.

Acknowledgment. The experiments were performed under the approval of the KEK-PF Program Review Committee (2001G092).

References and Notes

- Centi, G.; Ciambelli, P.; Perathoner, S.; Russo, P. *Catal. Today* **2002**, *75* (1–4), 3–15.
- Gates, B. C. *Chem. Rev.* **1995**, *95*, 511–522.
- Izumi, Y.; Chihara, T.; Yamazaki, H.; Iwasawa, Y. *J. Phys. Chem.* **1994**, *98*, 594–602.
- Izumi, Y.; Iwasawa, Y. *CHEMTECH* **1994**, *24* (7), 20–27.
- Izumi, Y.; Aika, K. *J. Phys. Chem.* **1995**, *99*, 10346–10353.
- Izumi, Y.; Kurakata, H.; Aika, K. *J. Catal.* **1998**, *175*, 236–244.
- Ali, A.; Alvarez, W.; Loughran, C. J.; Resasco, D. E. *Appl. Catal., B* **1997**, *14*, 13–22.
- Li, G.; Ichikawa, M.; Guo, X. *React. Kinetics Catal. Lett.*, **1996**, *59* (1), 75–86.
- Li, G.; Fujimoto, T.; Fukuoka, A.; Ichikawa, M. *J. Chem. Soc., Chem. Commun.* **1991**, 1337–1339.
- Kobylinski, T. P.; Taylor, B. W. *J. Catal.* **1974**, *33*, 376–384.
- Wakatsuki, Y.; Chihara, T. *Bull. Chem. Soc. Jpn.* **1999**, *72*, 2357–2363.
- Chihara, T.; Sawamura, K.; Ikezawa, H.; Ogawa, H.; Wakatsuki, Y. *Organometallics* **1996**, *15*, 415–423.
- Chihara, T.; Tase, T.; Ogawa, H.; Wakatsuki, Y. *Chem. Commun.* **1999**, 279–280.
- Ishiguro, A.; Liu, Y.; Nakajima, T.; Wakatsuki, Y. *J. Catal.* **2002**, *206* (1), 159–164.
- Ishiguro, A.; Nakajima, T.; Iwata, T.; Fujita, M.; Minato, T.; Kiyotaki, F.; Izumi, Y.; Aika, K.; Uchida, M.; Kimoto, K.; Matsui, Y.; Wakatsuki, Y. *Chem. Eur. J.* **2002**, *8* (14), 3260–3268.
- Hayward, C. T.; Shapley, J. R. *Inorg. Chem.* **1982**, *21*, 3816–3820.
- Eady, C. R.; Jackson, P. F.; Johnson, B. F. G.; Lewis, J.; Malatesta, M. C.; McPartlin, M.; Nelson, W. J. H. *J. Chem. Soc., Dalton Trans.* **1980**, 383–389.
- Yokoyama, T.; Hamamatsu, H.; Ohta, T. *EXAFSH 2.1*; The University of Tokyo.
- Based on X-ray crystallographic analysis of cluster 3. Unpublished work by T. Nakajima and Y. Wakatsuki.
- Binsted, N.; Cook, S. L.; Evans, J.; Greaves, G. N.; Price, R. J. *Am. Chem. Soc.* **1987**, *109*, 3669–3676.
- Wells, A. F. *Structural Inorganic Chemistry*, 5th ed.; Clarendon Press: Oxford, U.K., 1984.
- Basset, J. M.; Besson, B.; Choplin, A.; Thelier, A. *Philos. Trans. R. Soc. London A* **1982**, *308*, 115–124.
- Shen, J. G. C.; Liu, A. M.; Tanaka, T.; Ichikawa, M. *J. Phys. Chem. B* **1998**, *102*, 7782–7792.
- Platero, E. E.; de Peralta, F. R.; Parra, J. B. *J. Eur. Ceram. Soc.* **1998**, *18* (9), 1307–1312.
- Guglielminotti, E.; Boccuzzi, F. *J. Chem. Soc., Faraday Trans.* **1991**, *87* (2), 337–343.
- Davydov, A. A.; Bell, A. T. *J. Catal.* **1977**, *49* (3), 345–355.